INTERNATIONAL DESIGN CONFERENCE - DESIGN 2006
Dubrovnik - Croatia, May 15 - 18, 2006.

DESIGN 2006

INFLUENCE OF DIFFERENT GEAR LOAD MODELS ON CRACK PROPAGATION PREDICTIONS

S. Podrug and D. Jelaska

Keywords: moving load, gear tooth root, crack closure

1. Introduction

In conventional fatigue models of the gear tooth root it is usual to approximate actual gear load with pulsating force acting in the highest point of the single tooth contact. However, in actual gear operation, the magnitude as well as the position of the force, changes as the gear rotates through the mesh. A study to determine the effect of moving gear tooth load on crack propagation predictions was performed. Finite element method and linear elastic fracture mechanics theories are used for the simulation of the fatigue crack growth.

Moving load produces a non-proportional load history in a gear's tooth root. Consequently, the maximum tangential stress theory will predict a unique kink angle for each load increment, but herein crack's trajectory is computed at the end of the load cycle. An approach that accounts for fatigue crack closure effects is developed to propagate crack under non-proportional load.

2. Fatigue crack propagation

The application of the linear elastic fracture mechanics (LEFM) to fatigue is based upon the assumption that the fatigue crack growth rate, $\mathrm{d}a/\mathrm{d}N$, is a function of the stress intensity range $\Delta K = K_{max} - K_{min}$, where a is a crack length and N is a number of load cycles. In this study the simple Paris equation is used to describe the crack growth rate:

$$\frac{\mathrm{d}a}{\mathrm{d}N} = C\left[\Delta K(a)\right]^m \tag{1}$$

This equation indicates that the required number of loading cycles N_p for a crack to propagate from the initial length a_0 to the critical crack length a_c can be explicitly determined, if C, m and $\Delta K(a)$ are known. C and m are the material parameters and can be obtained experimentally, usually by means of a three point bending test. For simple cases the dependence between the stress intensity factor and the crack length $K = f(a)$ can be determined using the methodology given by [Ewalds and Wanhill, 1989]. For more complicated geometry and loading cases it is necessary to use alternative methods. In this work the FEM in the framework of the program package [FRANC2D, 2000], has been used for simulation of the fatigue crack growth.

Two gear models are being explored: first in which gear tooth was loaded with normal pulsating force acting at the highest point of the single tooth contact (HPSTC), and second one in which the fact that in actual gear operation the magnitude as well as the position of the force, changes as the gear rotates through the mesh is taken into account.

2.1 Model where load is approximated with force acting at the HPSTC

In most of recent investigations [Glodež *et al.*, 2002] a loading cycle of gear meshing is presumed as pulsating acting at the HPSTC (Figure 1.)

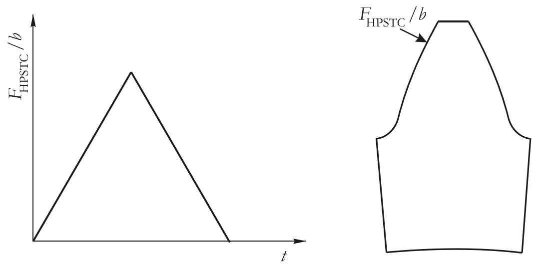

Figure 1. The pattern of loading cycle for the fatigue analysis

The initial crack is placed perpendicularly to the surface at the point where maximum principal stress occurs in a gear tooth root for load acting in the HPSTC. The threshold crack length a_0 below which LEFM is not valid, i.e. transition point between initiation and propagation period, may be estimated approximately as [Ostash *et al.*, 1999.]:

$$a_0 = \left(\frac{\Delta K_{\mathrm{th,eff}}}{\sigma_{\mathrm{D}}} \right)^2 \tag{2}$$

where $\Delta K_{\mathrm{th,eff}}$ is effective threshold stress intensity factor, and σ_{D} is fatigue limit.

The determination of the stress intensity factor (SIF) mode I and mode II is based on a *J* integral technique. The computational procedure is based on incremental crack extensions, where the size of the crack increment is prescribed in advance. In order to predict the crack extension angle the maximum tensile stress criterion (MTS) is used. In this criterion it is proposed that crack propagates from the crack tip in a radial direction in the plane perpendicular to the direction of greatest tension (maximum tangential tensile stress). The predicted crack propagation angle can be calculated by:

$$\theta_0 = 2\tan^{-1}\left[\frac{1}{4} \cdot \frac{K_{\mathrm{I}}}{K_{\mathrm{II}}} \pm \sqrt{\left(\frac{K_{\mathrm{I}}}{K_{\mathrm{II}}} \right)^2 + 8} \right] \tag{3}$$

The equivalent SIF is then:

$$K_{\mathrm{eq}} = \cos^2 \frac{\theta_0}{2} \left(K_{\mathrm{I}} \cos \frac{\theta_0}{2} - 3 K_{\mathrm{II}} \sin \frac{\theta_0}{2} \right) \tag{4}$$

A new local remeshing around the new crack tip is then required. The procedure is repeated until the equivalent SIF reaches the critical value K_{Ic}, when the complete tooth fracture is expected. Following the above procedure, one can numerically determine the functional relationship $K = \mathrm{f}(a)$.

In this paper, the stress intensity range in Paris equation is replaced by the effective stress intensity range:

$$\begin{aligned} \Delta K_{\mathrm{eff}} &= K_{\mathrm{eq,max}} - K_{\mathrm{cl}} \quad \text{for} \quad \mathrm{K}_{\mathrm{eq,min}} \le K_{\mathrm{cl}} \ , \\ \Delta K_{\mathrm{eff}} &= K_{\mathrm{eq,max}} - K_{\mathrm{eq,min}} \quad \text{for} \quad \mathrm{K}_{\mathrm{eq,min}} > K_{\mathrm{cl}} \ , \end{aligned} \tag{5}$$

where K_{cl} is SIF when closure occurs, and $K_{\mathrm{eq,max}}$ and $K_{\mathrm{eq,min}}$ are maximal and minimal SIFs during load cycle. For this gear load model $K_{\mathrm{eq,max}}$ is equal K_{eq} (4), and $K_{\mathrm{eq,min}} = 0$.

Effective range of SIF is calculated using model [Budiansky and Hutchinson, 1978] for plasticity induced crack closure, and influence of oxide induced crack closure, and roughness induced crack closure is taken into account by the concept of the partial crack closure, [Kujawski, 2002]:

$$\Delta K_{\mathrm{eff}} = K_{\mathrm{eq,\,max}} \left\{ 1 - \left(1 - 2\sqrt{1-\xi} \right) \left[1 + \left(\frac{2}{\pi} - 1 \right) g \right] \right\} \tag{6}$$

where g is a transition function:

$$g = \mathrm{e}^{-\left(\frac{K_{\mathrm{eq,\,max}}}{K_{\mathrm{th,max}}} - 1 \right)} \tag{7}$$

wher $K_{\mathrm{th,max}}$ is the maximum SIF at threshold, and ξ is normalized crack-wake plasticity, and it is estimated according to [Newman *et al.*, 2003], by fitting results from Budiansky and Hutchinson with 4th order polynomial:

$$\xi = 0{,}8561 + 0{,}0205R + 0{,}1438R^2 + 0{,}2802R^3 - 0{,}3007R^4 \tag{8}$$

where R is load ratio, $K_{\mathrm{eq,min}}/K_{\mathrm{eq,max}}$.

2.2 Moving force model

For moving force model, a quasi static numerical simulation method is presented in which the gear tooth engagement is broken down into multiple load steps and analyzed separately, [Lewicki *et al.*, 2000], [Spievak *et al.*, 2001].

During the contact of the teeth pair the load move along the each tooth flank and so changes its direction and intensity. In order to investigate the influence of moving load on the gear root stress amplitude, the analysis is divided, for example, in sixteen separated load cases (j = 0 to 15): Four of them take the force act on the tooth ahead (0 to 3) and four of them take the force act on the tooth after (12 to 15) the analyzed tooth; in six cases the entire load acts on the analyzed tooth (5-10), and in two cases the load is distributed on the two teeth in contact (4 and 11) (Figure 2.).

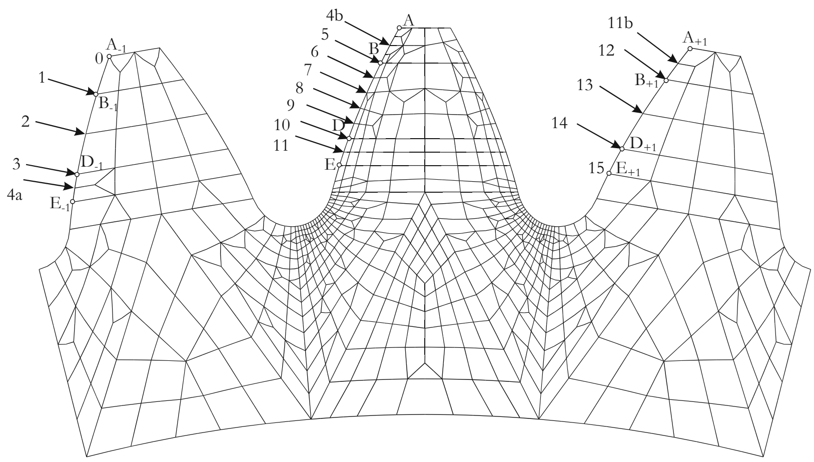

Figure 2. Load model

The initial crack is placed perpendicularly to the surface at the point where maximum principal stress occur in a gear tooth root for load acting in the HPSTC, and SIF history over one load cycle is computed. The moving load on the gear tooth is non-proportional, since the ratio of K_{II} to K_{I} changes during the load cycle. Consequently, the maximum tangential stress theory (3) will predict a unique kink angle for each load increment, but herein crack's trajectory is computed at the end of the load cycle.

The procedure is as follows:

(1) For load step from j-1 to j crack extension angle can be calculated according to MTS criterion (3):

$$\theta_{(j-1,j)} = 2\arctan\left[\frac{1}{4}\frac{K_{\mathrm{I}(j\max)}}{K_{\mathrm{II}(j\max)}} \pm \frac{1}{4}\sqrt{\left(\frac{K_{\mathrm{I}(j\max)}}{K_{\mathrm{II}(j\max)}}\right)^2 + 8}\right] \tag{9}$$

where $K_{\mathrm{I}(j\max)}$ and $K_{\mathrm{II}(j\max)}$ are SIFs for a load case which produce larger SIF mode I on corresponding interval.

(2) By means of calculated extension angles, combined stress intensity factor for j^{th} load case can be calculated (4):

$$K_{\mathrm{eq}(j)} = \cos^2\frac{\theta_{(j-1,j)}}{2}\left(K_{\mathrm{I}(j)}\cos\frac{\theta_{(j-1,j)}}{2} - 3K_{\mathrm{II}(j)}\sin\frac{\theta_{(j-1,j)}}{2}\right) \tag{10}$$

(3) Among them maximal $K_{\mathrm{eq,max}}$ need to be found (which there is always when load is in the HPSTC), in order to calculate SIF when closure occurs:

$$K_{\mathrm{cl}} = K_{\mathrm{eq,\,max}}\left(1 - 2\sqrt{1-\xi}\right)\left[1 + \left(\frac{2}{\pi} - 1\right)g\right] \tag{11}$$

(4) From Paris equation crack extension after one load cycle is:

$$\mathrm{d}a_{\mathrm{c}} = C\left(K_{\mathrm{eq,\,max}} - K_{\mathrm{cl}}\right)^m \tag{12}$$

(5) Since crack propagates only when $K_{\mathrm{eq}(j)} > K_{\mathrm{cl}}$, so for those load steps crack extension is calculated. The amount of extension between load steps is proportional to the ratio of the change in equivalent SIF to the effective SIF

$$\mathrm{d}a_{(j-1,j)} = \frac{K_{\mathrm{eq}(j)} - K_{\mathrm{eq}(j-1)}}{2\left(K_{\mathrm{eq,\,max}} - K_{\mathrm{cl}}\right)}da_{\mathrm{c}} \tag{13}$$

(6) In order to ensure that entire cycle part from crack opening to the crack closure participate in crack extension, the intersection between K_{cl} and $K_{\mathrm{eq}(j)}$ curves need to be determined. When load step for which $K_{\mathrm{eq}(j\text{-}1)} < K_{\mathrm{cl}} < K_{\mathrm{eq}(j)}$ is determined, then $K_{\mathrm{eq}(j\text{-}1)} = K_{\mathrm{cl}}$, respectively when load step for which $K_{\mathrm{eq}(j\text{-}1)} > K_{\mathrm{cl}} > K_{\mathrm{eq}(j)}$ is determined, then $K_{\mathrm{eq}(j)} = K_{\mathrm{cl}}$. As result after one load cycle crack trajectory is obtained, and is schematically presented in Figure 3., assuming the load cycle has been discretized into four steps.

(7) The final crack trajectory is approximated by a straight line from the initial crack tip location to the final crack growth location. The straight line approximation has length da_{c}, and its orientation is defined by the final angle θ_{f}

$$\theta_{\mathrm{f}} = \arctan\frac{\sum \mathrm{d}a_{(j-1,j)}\sin\theta_{(j-1,j)}}{\sum \mathrm{d}a_{(j-1,j)}\cos\theta_{(j-1,j)}} \tag{14}$$

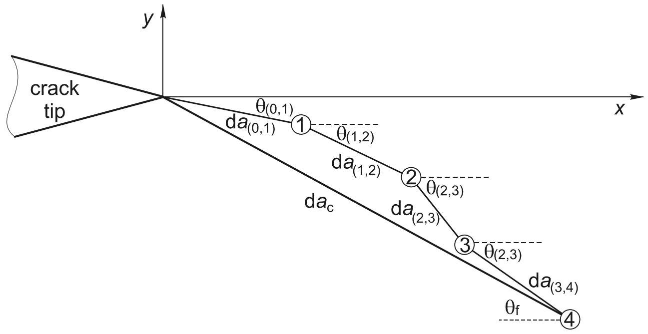

Figure 3. Schematic of crack extension after one load cycle

Since crack extension over one load cycle is too small to update geometry model, the crack will be extended in θ_f direction with previously determined crack increment size. Finally, the crack path and number of loading cycles for the crack propagation to the critical length are estimated.

3. Practical examples

The crack propagation was analyzed on the gear wheel of the gear pair 1 (GP1), and on the pinion of the gear pair 2 (GP2) [Lewicki and Ballarini, 1997], with basic data given in Table 1.

Table 1. Basic data of studied gears

Title	Symbol	**Gear pair 1**	**Gear pair 2**
Number of teeth 1	z_1	11	28
Number of teeth 2	z_2	39	28
Module	m, mm	4,5	3,175
Addendum modification coefficient 1	x_1	0,526	-0,05
Addendum modification coefficient 2	x_2	0,0593	-0,05
Gear width 1	b_1, mm	32,5	6,35
Gear width 2	b_2, mm	28	6,35
Flank angle of tool	α_n	24°	20°
Radial clearance factor	c^*	0,35	0,35
Relative radius of curvature of tool tooth	ρ_f^*	0,25	0
Addendum of tool	h_a^*	1	1,05
Dedendum of tool	h_f^*	1,35	1,35
Tip diameter	d_a	Standard clearance	Standard tooth height

The GP1 were made of high strength alloy steel 42CrMo4, and the GP2 were made of high strength alloy steel 14 NiCrMo 13-4, case carburized and ground. The teeth of the GP2 were hardened to a case hardness of 61 HRc (710 HV), and a core hardness of 38 HRc (375 HV), and the effective case depth (depth at a hardness of 50 HRc (550 HV)) was 0,78 mm. Material parameters are given in Table 2.

Using material parameters (Table 2) and equations (2), and (6), the initial crack length for GP1 is estimated to be 200 μm. Since crack increment size need to be prescribed in advance, crack increment size is taken to be 0,2 mm up to the crack length $a = 4$ mm, and after this 0,4 mm to the critical crack length. For GP2 the initial crack length is estimated to be 10 μm, and crack increment size is taken to be 5 μm up to the crack length $a = 25$ μm, and after this 25 μm up to the crack length $a = 0{,}2$ mm, and after this 0,1 mm to the critical crack length.

Table 2. Material parameters

		C, $\frac{\text{mm}}{\text{cycles}\times\left(\text{MPa}\sqrt{\text{mm}}\right)^m}$	m	ΔK_{th}, $\text{MPa}\sqrt{\text{mm}}$	K_{Ic}, $\text{MPa}\sqrt{\text{mm}}$
GP1	42 Cr Mo 4 AISI 4142	$3{,}31\cdot10^{-17}$	4,16	269	2620
GP2	14 NiCrMo 13-4 AISI 9310	$3{,}128\cdot10^{-13}$	2,954	122	2954

Since it was believed that tooth bending fatigue cracks in GP2 would be difficult to initiate, a notch were fabricated in the fillet region to promote crack initiation (Figure 4.) [Lewicki and Ballarini, 1997].

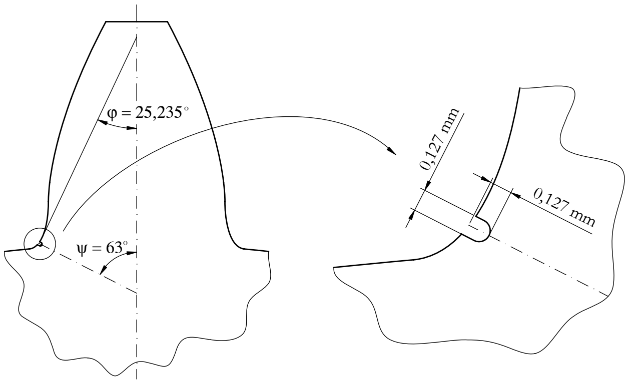

Figure 4. Notch position and dimensions for GP2

Differences in crack paths for two gear models for gear wheel of the GP1 are shown in Figure 5a., and differences in number of loading cycles for the crack propagation to the critical length, for different values of nominal torque transmitted by the gear set, are shown in Figure 5b.

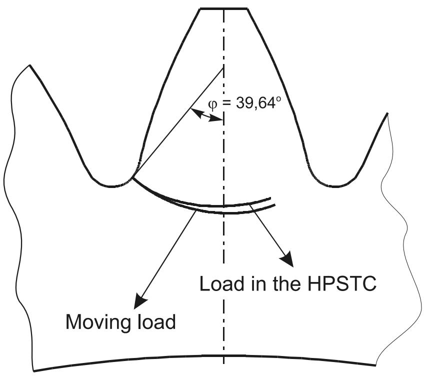

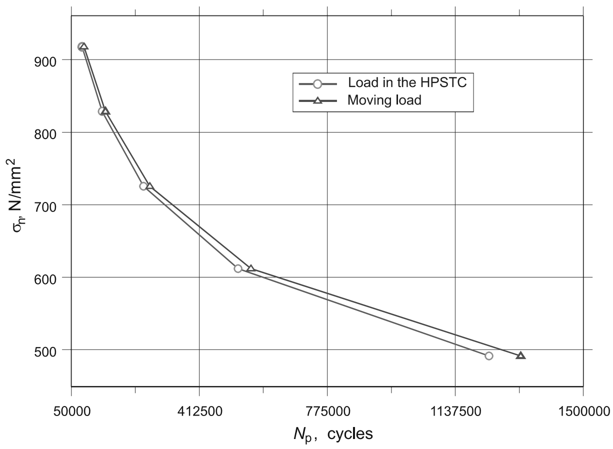

Figure 5. a) Comparison of crack paths **Figure 5. b) Comparison of crack propagation lives**

Differences in crack paths for two gear models for pinion of the GP2 are shown in Figure 6a, and differences in number of loading cycles for the crack propagation to the critical length are shown in Figure 6b. In Figure 6a. A denotes crack path obtained numerically with load acting at the HPSTC, B denotes crack path obtained with moving force model, and C is experimentally obtained crack path. Nominal torque for this gear set was 135,664 Nm.

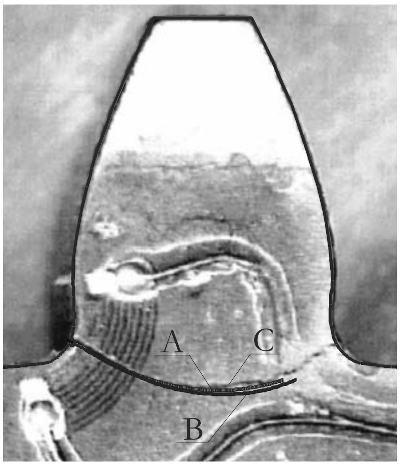

Figure 6. a) Comparison of crack paths

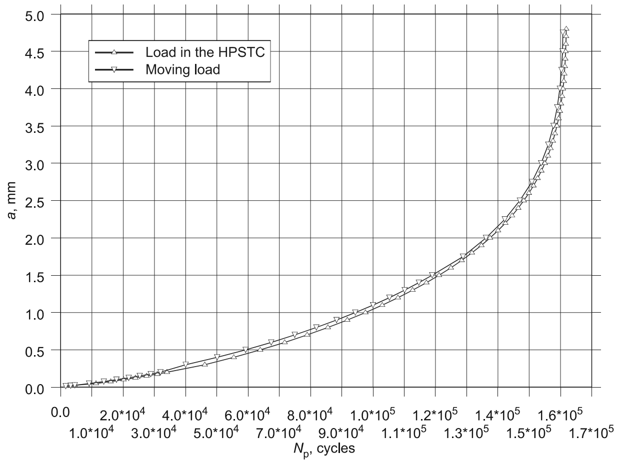

Figure 6. b) Comparison of crack propagation lives

In Figure 7. number of loading cycles for the crack propagation obtained with moving force model is compared with number of loading cycles for the crack propagation obtained experimentally.

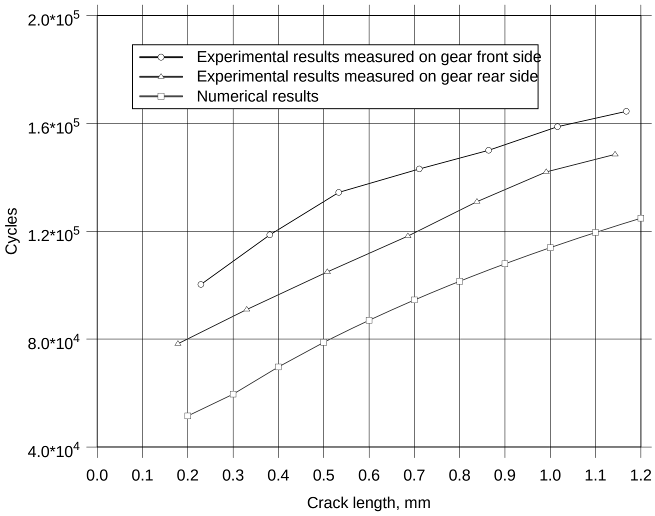

Figure 7. Comparison of crack propagation lives obtained experimentally and numerically

4. Conclusion

Observed differences in crack paths and number of loading cycles for the crack propagation to the critical length, obtained with two gear load models, are larger for gear pair 1 then for gear pair 2.

Reason for that is primarily in contact ratio ε_a, which is considerably smaller for gear pair 1 ($\varepsilon_{\alpha,1} = 1,256$) then for gear pair 2 ($\varepsilon_{\alpha,2} = 1,740$). This means longer period of single tooth contact, causing flatter distribution of equivalent SIF during one load cycle.

Flatter distribution of equivalent SIF means that in addition to force acting in the HPSTC, also neighboring load steps has significant impact on crack growth, because they values are higher then

value of SIF when closure occurs, and because of nonproportional load each load step propagates crack into different direction.
Gear pair 2 has sharp stress distribution over one load cycle, and because of that influence of load steps around HPSTC is small, and crack path is primarily influenced by the load acting in the HPSTC.
Crack closure effect is also taken into account, extending analitical model for plasticity induced crack closure with partial crack closure concept. In this way two other closure mechanisms: roughness and oxide induced crack closure are taken into account.
By so completed numerical procedure, the predictions of crack propagation lives and crack paths in regard to the gear tooth root stresses are obtained, which are significantly closer to experimental results then existing methods.

References

Budiansky, B., Hutchinson, J.W., "Analysis of Closure in Fatigue Crack Growth", Journal of Applied Mechanics, 45, 1978, pp. 267-276.

Ewalds, H. L, Wanhill, R. J., "Fracture Mechanics", Edward Arnold Publication, London, 1989.

FRANC2D, "User's Guide", Version 2.7, Cornell University, 2000.

Glodež, S., Šraml, M., Kramberger, J.,"A Computational Model for Determination of Service Life of Gears", International Journal of Fatigue, 24(10), 2002, pp. 1013-1020.

Kujawski, D., "Utilization of Partial Crack Closure for Fatigue Crack Growth Modeling", Engineering Fracture Mechanics, 69, 2002, pp. 1315-1324.

Lewicki, D.G., Ballarini, R., Rim Thickness Effects on Gear Crack Propagation Life, International Journal of Fatigue, 87, 1997, pp. 59-86.

Lewicki, D.G., Spievak, L.E., Handschuh, R.F., Consideration of Moving Tooth Load in Gear Crack Propagation Predictions, NASA/TM-2000-210227, 2000.

Newman, J.A., Riddell, W.T., Piascik, R.S., "A Threshold Fatigue Crack Closure Model: Part I – Model Development", Fatigue Fract Engng Mater Struct, 26, 2003, pp. 603-614.

Ostash, O.P., Panasyuk, V.V., Kostyk, E.M., Assessment of the Period to Fatigue Macrocrack Initiation Near Stress Concentrators by Means of Strain Parameters, Fatigue Fract Engng Mater Struct, 22, 1999, pp. 687-696.

Spievak, L.E., Wawrzynek, P.A., Ingraffea, A.R., Lewicki, D.G., Simulating Fatigue Crack Growth in Spiral Bevel Gears, Engineering Fracture Mechanics, 68, 2001, pp. 53-76.

Dr. sc. Srđan Podrug
Assistant Professor
FESB / University of Split, Department of Mechanical Engineering and Naval Architecture
R. Boškovića bb, Split, Croatia
Tel.: 021-305-873
Fax.: 021- 463-877
Email: spodrug@fesb.hr
URL: *http://www.fesb.hr/~spodrug*